sustainability

MDPI

Article

Iron Removal from Quartz Ore by Acid Leaching: From Lab- to Pilot-Scale

Svetlana Zueva *, Valentina Innocenzi, Nicolò Maria Ippolito, Ionela Birloaga, Francesco Vegliò and Francesco Ferella

Department of Industrial and Information Engineering and Economics, University of L'Aquila, Monteluco di Roio, 67100 L'Aquila, Italy; valentina.innocenzi@univaq.it (V.I.); nicolomaria.ippolito@univaq.it (N.M.I.); ionelapoenita.birloaga@univaq.it (I.B.); francesco.veglio@univaq.it (F.V.); francesco.ferella@univaq.it (F.F.)
* Correspondence: svetlana.zueva@univaq.it; Tel.: +39-0862-434236

Abstract

Quartz in high-purity form, i.e., with an iron content <100 mg/kg, has valuable properties such as superior UV transmission, thermal stability, and resistance to devitrification, which are highly useful for optical applications. In this study, acid leaching was tested to optimize the production of optical-grade quartz from mined quartz, transforming an environmentally polluting process into a sustainable one, aligning with several United Nations Sustainable Development Goals (SDGs). Initially, when iron removal was obtained with direct, cross-current, and counter-current leaching methods, the results were unsatisfactory. However, a variation consisting of incorporating sulfuric acid regenerated via membrane filtration into the typical counter-current scheme was proven effective, reducing acid consumption and enhancing water recycling in the process, mitigating the environmental impact. The best optimized combination was the three-step counter-current method, with acid regeneration and fresh make-up after each cycle. The conditions were temperature 90 °C, solid-to-liquid ratio 30% wt/vol, time 3 h, and H_2SO_4 concentration of 1 M. The iron extraction yield was close to 89%.

Keywords: iron; acid leaching; optical quartz; process optimization; acid recycling

check for updates

Academic Editor: Roberta Palmieri

Received: 28 September 2025
Revised: 2 November 2025
Accepted: 3 November 2025
Published: 9 November 2025

Citation: Zueva, S.; Innocenzi, V.; Ippolito, N.M.; Birloaga, I.; Vegliò, F.; Ferella, F. Iron Removal from Quartz Ore by Acid Leaching: From Lab- to Pilot-Scale. *Sustainability* **2025**, *17*, 10008. https://doi.org/10.3390/su172210008

Copyright: © 2025 by the authors. Licensee MDPI, Basel, Switzerland. This article is an open access article distributed under the terms and conditions of the Creative Commons Attribution (CC BY) license (https://creativecommons.org/licenses/by/4.0/).

1. Introduction

In recent years, high-purity quartz (HPQ) has been recognized as a strategically significant resource [1]. Depending on SiO_2 content, it can be classified into four groups by purity grade [2]: ultra-high (>99.998%), high (>99.995%), medium (>99.99), and standard (>99.9).

HPQ with a SiO_2 content greater than 99.995% widely used in environmentally beneficial technologies such as solar panels [3]. But its extraction and refinement can pose significant environmental and social challenges if not managed responsibly. Moreover, the diminishing availability of natural crystals suitable for producing high-purity quartz has created an urgent need to develop innovative and efficient methods for obtaining this material from alternative sources. One promising approach involves the extraction and beneficiation of silica from quartz sand.

However, a significant obstacle remains: quartz sand contains iron, one of the most persistent and challenging impurities to remove. The iron content is a key factor determining the suitability of quartz for various applications, as it greatly affects both its color and performance characteristics. For instance, quartz intended for semiconductor applications

requires an exceptionally low iron concentration—typically less than 1.0 ppmw [4]. The removal of iron is, therefore, a critical step in the processing of high-quality quartz products.

Quartz purification methods are generally divided into two categories: physical and chemical purification. When iron exists as an independent mineral (e.g., goethite, hematite, limonite, ilmenite, magnetic pyrite, etc.), it can be separated from quartz using physical methods such as gravity separation [5], flotation [6], and magnetic separation [3,7,8]; or through combined methods such as gravity–magnetic separation [9]; or a combination of indirect ultrasound irradiation with reverse flotation and magnetic separation, based on differences in density, surface, and magnetic properties [10].

Commonly used pre-treatment operations include crushing, grinding, grading, and optical sorting. In some cases, iron oxide films adhere to the surface of quartz, or iron-containing minerals occur within quartz particles in a diffuse state, existing as a solid solution. In case of surface contamination, scrubbing with diluted acids or alkalis effectively removes impurities and prevents interference in subsequent purification processes [11]. But when iron ions (Fe^{2+} and Fe^{3+}) are present as inclusions within the quartz lattice, substituting for silicon, chemical leaching [12], or high-temperature calcination [13] is required. The last one can effectively remove gas–liquid inclusions in quartz crystals and drive impurity ions to the surface, facilitating subsequent purification. Nevertheless, it is a highly energy-intensive and poorly scalable process.

The manufacturing processes for high-purity quartz are relatively expensive due to energy consumption and the use of a huge amount of chemicals. Therefore, optimizing these processes is essential for enhancing competitiveness in this sector. Nowadays, chemical methods are the most used in the mining industry. While many researchers have successfully studied lab-scale de-ironing from quartziferous ores, there is a lack of studies at a larger scale, such as in pilot plants. Most existing processes have not been optimized or integrated, leading to higher operating costs. However, iron is not the only impurity that needs to be removed from sand or quartz-containing ores to produce high-purity quartz [14] or whitening minerals [15].

Various strategies were explored to obtain high-purity quartz (HPQ), an essential mineral resource for key sectors including photovoltaics, semiconductors, optical fibers, space exploration, and aeronautics [16–18]. Mechanochemical activation is an effective technique which had a whitening effect on minerals, with excellent results [19].

As mentioned, HPQ is a crucial foundational material for emerging strategic industries. For instance, due to resource shortages in China and relatively outdated purification technology, more than 90% of high-purity quartz raw materials are imported from other countries [20].

Therefore, circularity in this sector should aim to recycle as much HPQ as possible, utilizing strategies and best environmental practices that have been established in other sectors, such as demolition waste and recycled concrete aggregates [21,22].

To achieve high iron extraction yields, high temperatures (80–90 °C) [23] and extended processing times (3 to 5 h) are typically required [24]. Ubaldini et al. [24] conducted tests on continuous leaching using a fixed-bed reactor containing quartz sand, where they recycled an oxalic acid solution while testing several operating parameters. The greatest iron reduction achieved was 46%, with a final Fe_2O_3 concentration of 0.0163% wt. The mechanism may involve complexation and reduction of Fe(III) to Fe(II).

Furthermore, oxalic acid was used with H_2SO_4 in a rotary drum reactor. Under optimal operating conditions, the iron concentration was reduced from 0.0259% to below the target value of 0.015% as Fe_2O_3. Oxalic acid exhibited high yields in removing iron from a red clay, lowering Fe_2O_3 to 3.64% wt, namely a reduction of 78.7%, which makes it

useful for ceramic manufacturing [25]. The kinetics of the dissolution process were also assessed [26].

In addition to oxalic acid, other reducing agents such as citric acid and glucose were tested in conjunction with sulfuric acid, i.e., glucose and citric acid. However, oxalic acid outperformed the others by achieving a 99% iron dissolution. The yields with citric acid and glucose were consistently above 70% [27].

Arslan V. investigated ultrasound-assisted acid leaching in diluted hydrochloric and oxalic acids [28]. Under the optimum conditions, iron removal was determined to be 95.08%. The author managed to reduce the Fe_2O_3 content from 0.225 to 0.011% with 95.08% removal efficiency, increasing the SiO_2 concentration from 97.841 to 99.907%.

Ibrahim A.F.M. et al. applied distilled water attrition scrubbing and screening over a 25 µm sieve, and then leaching using a mixture of equal amounts of phosphoric and oxalic acids [29]. The head sample shows a silica and iron oxide content of 95.69% and 2379 ppm, respectively. Attrition and separation over a 25 µm sieve increase the silica content from 95.69 to 97.05% and decrease the residual iron oxide from 2379 to 455 ppm. The final product after leaching had 99.82% silica and 55 ppm iron oxide.

Roasting is an effective pre-treatment for quartz ore when combined with $(NH_4)_2SO_4$, which helps reduce Fe(III) to Fe(II) at temperatures between 400 °C and 500 °C for 1.5 h in an airflow environment. Following this process, leaching with a solution of 5% wt H_2SO_4 and 10% wt HF can lower the Fe_2O_3 content from an initial concentration of 145 mg/kg to below 0.3 mg/kg [30].

High-temperature roasting, conducted at temperatures ranging from 600 °C to nearly 1200 °C, can alter the crystalline structure of quartz, thereby enhancing the effectiveness of the acid in removing iron and other impurities. In one procedure, iron extraction was about 99% from quartz that underwent magnetic separation, followed by roasting at 900 °C for 4 h, and subsequently autoclave leaching with an HCl and $H_2C_2O_4$ solution at 200 °C for 6 h [31]. However, this method has the drawback of high energy costs associated with both the thermal and leaching stages, which last a total of about 10 h.

Moreover, reducing iron content is essential when utilizing high-silica iron ore tailings as feedstock to recover high-purity quartz with a purity of 99.99%. This can be achieved through high-intensity magnetic separation, followed by a two-stage leaching process using a mixture of H_3PO_4, HCl, and HF, which can reduce the iron oxide content by nearly 91% [3].

HF enhances the removal process by dissolving the surface of quartz particles and penetrating small, narrow channels. This allows the contact between iron and other metal particles embedded inside the quartziferous grains. However, the use of HF presents significant corrosion challenges in industrial facilities that process thousands of tons of quartz each year. Zhang et al. [31] compared the effectiveness of different acids—i.e., H_2SO_4, $H_2C_2O_4$, phosphoric H_3PO_4, HCl, and HF—for whitening quartziferous ore and sand by ultrasounds. They achieved a 77% reduction in iron content using phosphoric acid from an initial concentration of 481 mg/kg of Fe_2O_3. However, this outcome was obtained with a solid-to-liquid ratio (S/L) equal to 5% wt/vol, which is relatively low. Increasing the S/L ratio to 20% wt/vol, the extraction of Fe_2O_3 decreased to 46%.

Bioleaching was also used for quartz whitening. While its kinetics are generally slower than those of conventional chemicals like mineral and organic acids, Styriakova et al. [32] reported a 50% removal of Fe_2O_3 after 83 days of treating quartz with heterotrophic bacteria in a pilot plant. This experiment confirmed laboratory-scale results obtained with samples from three different Slovakian sites; after 83 days, the iron oxide removal was 50%, 47%, and 30% [33].

Despite numerous works in this area, there is a significant gap in the current literature regarding the enhancement of environmental sustainability and economic viability in producing HPQ. Indeed, most of the processes listed above are primarily aimed at increasing quartz purity. This study aimed to develop an efficient process of obtaining HPQ with Fe_2O_3 concentration below 100 mg/kg, aligned with the SDGs, minimizing the environmental footprint associated with its production.

This study presents an optimized process with the key aspect of maximizing acid and water recycling. This sustainable approach not only lowers operating costs but also significantly mitigates the environmental impacts linked to the consumption of natural resources. From the perspective of sustainable development principles, this approach represents transforming an environmentally polluting process into a sustainable one (Figure 1). In other words, it contributes to the achievement of several of the 17 United Nations Sustainable Development Goals (SDGs) [34], including the following:

1. Sustainable management of water resources throughout industrial processes (SDG 6).
2. Development of innovative technologies for sustainable industrialization (SDG 9).
3. Implementation of the circular economy and recycling. Processing secondary products reduces the need for mineral extraction and decreases environmental impact (SDG 12).
4. Reducing CO_2 emissions associated with quartz mining and processing (SDG 13). Reducing emissions and using low-carbon logistics. Quartz-based products (such as solar panels) help mitigate the effects of climate change.

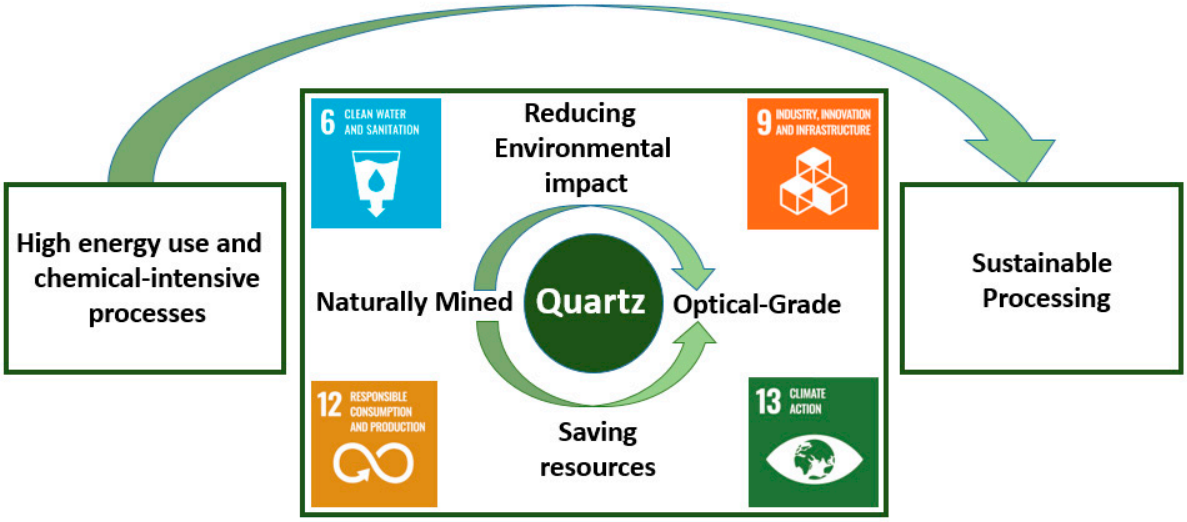


Figure 1. Sustainable HPQ production aligned with the Sustainable Development Goals (SDGs).

The findings of this study illustrate how innovative practices can lead to a dual benefit: enhancing the economic viability of quartz production while safeguarding environmental integrity. Thus, this study not only paves the way for advancements in quartz production but also champions the broader global agenda for sustainability as set forth by the SDGs. Integrating these sustainable practices can ensure that the optical quartz industry contributes to technological progress while minimizing its ecological footprint.

2. Materials and Methods

The experimental campaign was conducted using a sample particle size lower than 1200 µm, as supplied by a Turkish company. The sample was ground by a ball mill and sieved to −150 µm for digestion in a mixture of aqua regia and HF. After that, one gram of the sample was digested in 50 mL of aqua regia ($HCl:HNO_3$ = 3:1) in a mechanically stirred digestion bomb. After 3 h, the suspension was filtered and diluted to 1:100 in a

calibrated flask with deionised water. The exact iron content of the sample (668 mg/kg) was determined by Atomic Absorption Spectrometry (AAS) using a SpectrAA 200 spectrometer (Varian, Inc., Palo Alto, CA, USA).

Table 1 represents the weight percentage of the quartz sample according to an X-ray Fluorescence (XRF) analysis, where only the most concentrated elements are listed.

Table 1. XRF analysis of the quartz sample.

Element	Concentration (% wt)
Al	0.6368
Si	44.40
P	0.0264
S	0.0207
K	0.1096
Ca	0.0312
Ti	0.0500
Cr	0.0187
Fe	0.1200
Zr	0.4499

Leaching trials were conducted in 250 mL flasks, which were placed in a water bath (BSD/D, ISCO) and stirred at 200 rpm, unless stated otherwise. Three experimental configurations were investigated:

1. Direct Leaching: A 2^5 full factorial design was used to investigate the effects of the solid-to-liquid (S/L) ratio, concentration of sulfuric acid (H_2SO_4), time of reaction, wash water volume, and temperature.
2. Cross-Current Configuration: In this approach, the leach liquor was recycled back to leach two other quartz samples in a three-step process. Fresh H_2SO_4 was added to restore the solution volume to its initial amount.
3. Counter-Current Leaching Configuration: This method also employed a three-step process.

Leaching tests were performed with 200 rpm stirring. A total of 10 g of the as-received quartz sample (<1200 μm particle size) was immersed in 100 mL solutions of sulfuric acid. All the solutions after leaching (Spent Leaching Solutions—SLS) were subjected to chemical analysis with AAS for their Fe content determination. Considering their final volume, initial sample concentration, and the achieved Fe concentration, the efficiency of the procedure for each run was determined.

3. Results

To properly assess and optimize the removal of iron from a waste material, it is necessary to conduct well-designed experiments. A 2^5 full factorial design for acid leaching parameters, combined with different leaching strategies (direct leaching Figure 2a, cross-current leaching Figure 2b, and counter-current leaching Figure 2c), was studied to provide a comprehensive and systematic approach. Here is a breakdown of the necessity and rationale behind each component.

Direct leaching was chosen for the full factorial design of acid leaching parameters because it provides a simple, controlled, and representative system to systematically evaluate how each factor and its interactions influence iron removal from the waste material. It did help to understand the leaching chemistry and reaction kinetics before testing more complex setups like cross-current or counter-current systems.

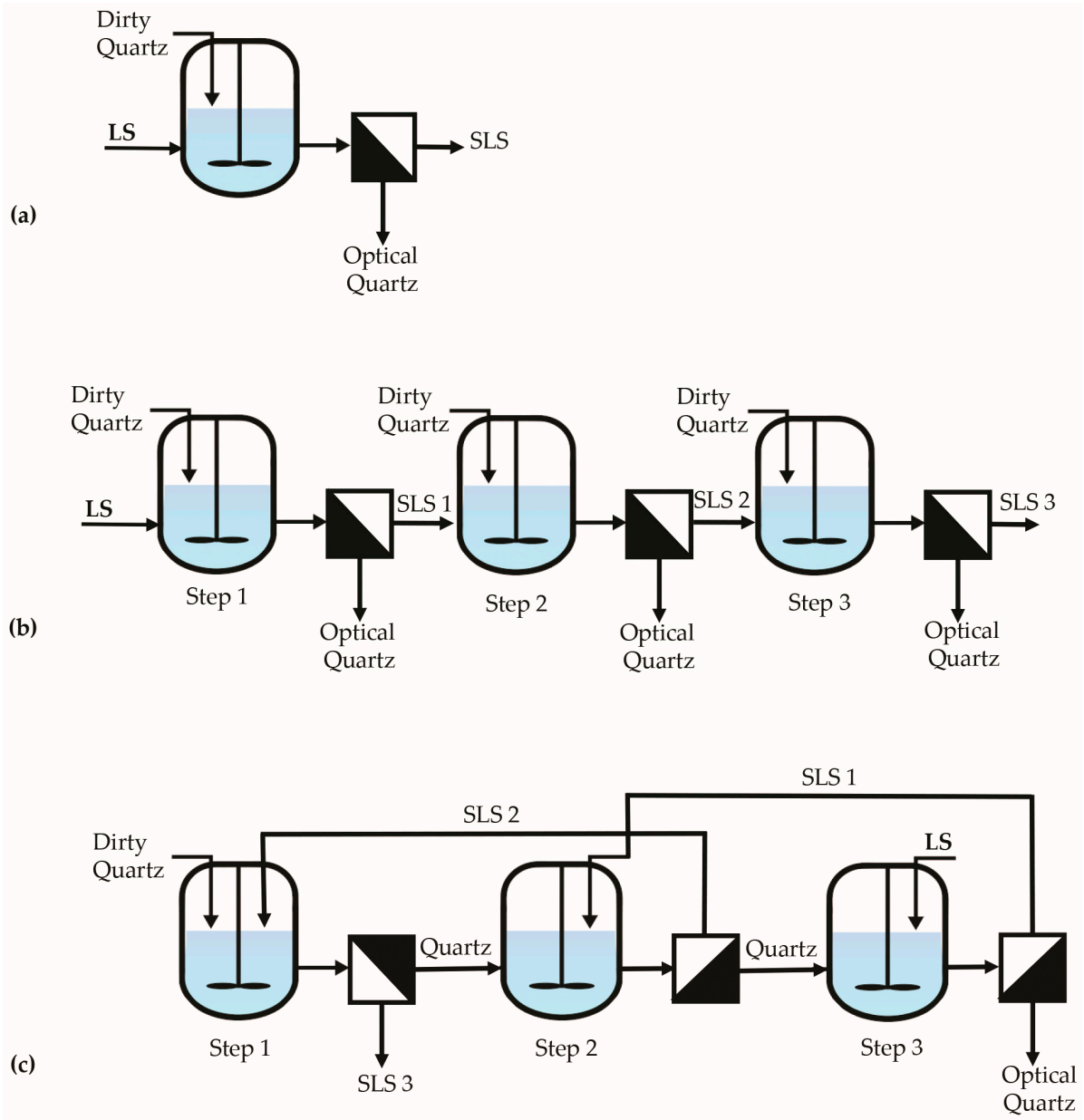


Figure 2. Schematic of experimental leaching configurations: (**a**) direct; (**b**) cross-current; (**c**) counter-current.

After that, optimized parameters were applied in cross-current and counter-current leaching, helping assess scalability and reagent efficiency under more realistic conditions.

3.1. Lab Scale Acid Leaching

3.1.1. Direct Leaching

Sulfuric acid was selected for the leaching process since it has some advantages over the other two strong inorganic acids (HCl and HNO_3): first of all, it does not fume, does not produce hazardous fumes like HNO_3 during reaction, and it is economical with respect to the others.

Previous studies have demonstrated that the key parameters influencing leaching efficiency are temperature, acid concentration, particle size, and the solid-to-liquid ratio [35,36]. Kefaifi et al. [35] reported that acid concentration exerts a more significant effect on achieving the desired silica purity than either particle size or leaching duration.

In the present study, besides temperature, leaching time, acid concentration, and solid-to-liquid ratio, the influence of washing water was also evaluated through ANOVA

analysis (Table 2). The 2^5 full factorial design involved 32 treatment combinations and three replications of the central point, with a goal of good estimation of the experimental error.

Table 2. Factors investigated and relevant levels.

Factor	Variable	Level		
		Low (−)	Medium (0)	High (+)
A	Solid concentration (% wt/vol)	10	20	30
B	H_2SO_4 concentration (mol/L)	1	1.5	2
C	Leaching time (h)	1	2	3
D	Wash water (% of initial solution volume)	30	40	50
E	Leaching temperature (°C)	70	80	90

This factorial plan was worked out by the analysis of the variance (ANOVA) according to the Yates algorithm, and the main effects among independent variables and their interactions with significance greater than 95% have been plotted in Figure 3.

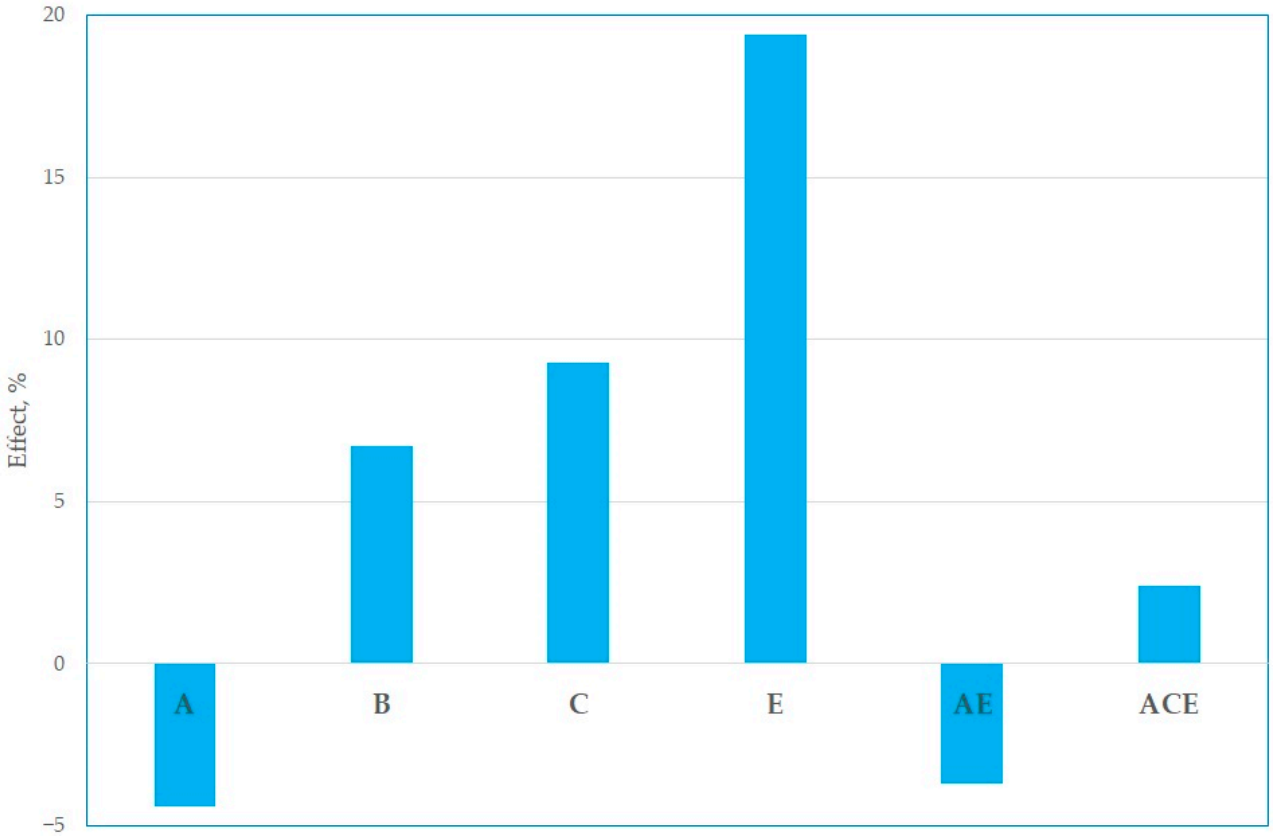


Figure 3. Effects of main factors and their interactions.

As can be noted, the most significant positive factors are sulfuric acid concentration (B), process time (C), and leaching temperature (E). Their increment determines the increase in Fe extraction yield by around 7, 8, and 15%, respectively. Another significant independent variable was solid concentration (A), which had a negative effect; a greater solid concentration determined the reduction in iron extraction by approximately 8%.

In addition to these parameters, other positive (ACE) and negative (AE) interactions were observed. The results indicated that iron dissolution was adversely affected by the

solid concentration; however, this effect could be mitigated by extending the process duration from 1 to 3 h. In the case of a 30% solid load, this adjustment led to an increase in the Fe extraction yield from 62.3% to 76.6%. Indeed, the greatest extraction yield (80.5%) was achieved in a test with 10% wt/vol solid-to-liquid (S/L) ratio, 2 mol/L sulfuric acid concentration in 3 h at 90 °C by using 50 mL of washing water (WW) (50% of the starting volume of the leaching solution) of water to wash the quartz cake recovered by filtration at 0.45 µm.

Hence, if the iron concentration must be reduced from the initial 668 ppm to below 100 ppm, the leaching process can be considered effective when the extraction yield is at least 85%.

3.1.2. Cross-Current Leaching

For a better sustainability of the process, the pregnant solution was reused to leach two new quartz samples (cross-current process, Figure 2b) in the same experimental conditions; the pregnant solution volume was brought back to its initial volume after each step with a make-up of fresh sulfuric acid solution (2 mol/L). The results are listed in Table 3.

Table 3. Extraction yields of the 3-stage cross-current leaching process (H_2SO_4 2M, S/L 10% wt/vol., temperature 90 °C, time 3 h).

Step		Fe Concentration (mg/L)	Extraction Yield (%)	Total Extraction (%)
1	SLS	192	79.8	80.4
	Wash water	4.2	1.6	
2	SLS	287	49.5	62.1
	Wash water	35.5	12.6	
3	SLS	335	8.6	26.7

From Table 3, it can be noted that the efficiency of the leaching process was low, especially when the solution was reused for the third time. Therefore, further experiments were continued in the counter-current leaching.

3.1.3. Counter-Current Leaching

Other tests were conducted in a three-stage counter-current process in order to reduce the consumption of sulfuric acid, since the concentration required to obtain the optical grade by direct leaching was rather high (2 mol/L), and this results in a huge consumption and relevant cost of sulfuric acid. The counter-current scheme is shown in Figure 4. The experiments were started with a direct leaching (Figure 4a), after which the resulting solutions (LS2 and LS3) were reused for the first cycle of the counter-current leaching procedure (Figure 4b).

The counter-current leaching tests were conducted in the following conditions: 1 M H_2SO_4, S/L 10% wt/vol, 90 °C, duration 1.5 h for each step, 90 °C, 50% of washing water volume, and make-up of each stage with 1M H_2SO_4 solution.

Further, a second cycle was performed with solution coming from the second and third steps of the first cycle for the leaching of a new solid. A fresh solution was used for the third leaching step of every cycle. It is worth mentioning that when the solutions were reused, their volume was always brought back to the desired volume with a fresh solution of the same concentration. The results achieved for the first three cycles are shown in Table 4.

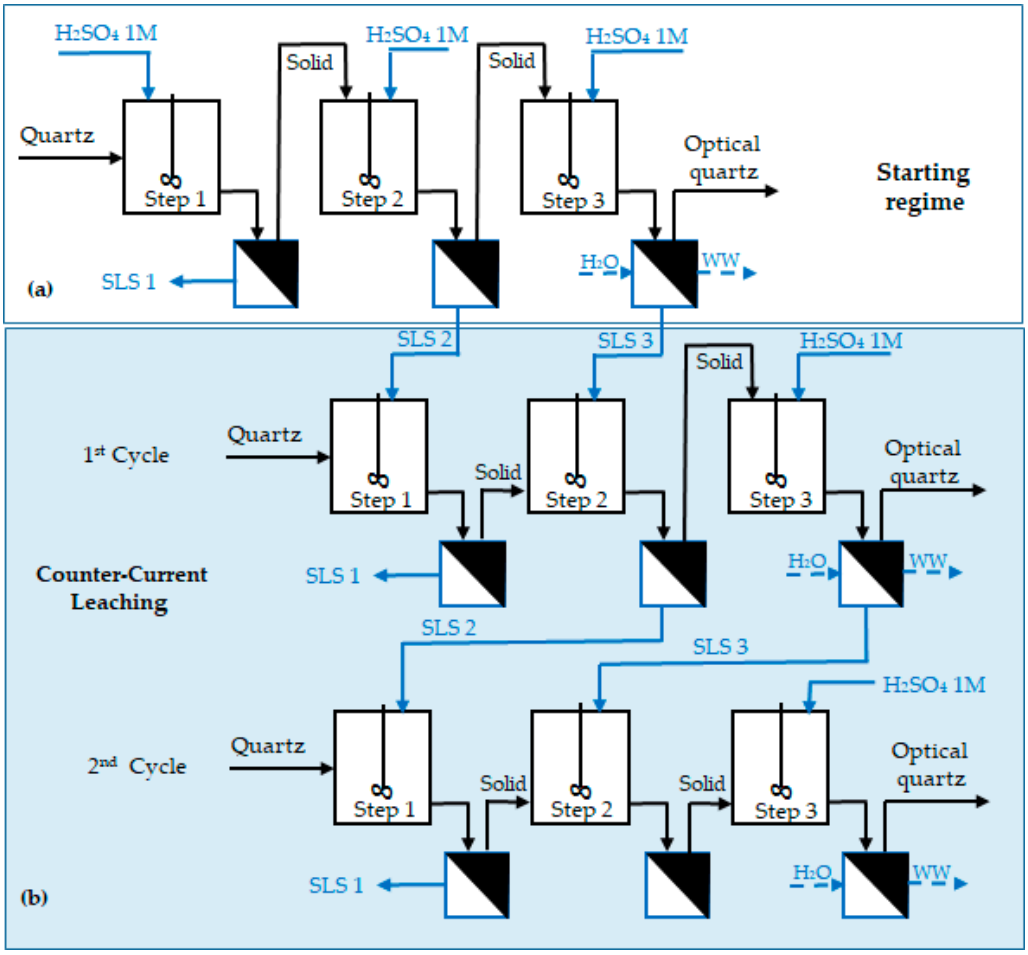


Figure 4. Schematic of the leaching tests conducted using the counter-current methodology: (**a**) starting regime; (**b**) counter-current leaching.

Table 4. Extraction yields of the 3-stage counter-current leaching process.

Cycle	Step		Fe Concentration (mg/L)	Extraction Yield (%)	Total Extraction (%)
	Starting regime				
	1		140.8	65.3	80.6
	2		54.1	12.8	
	3		15.4	1.9	
	Washing water		5.8	0.6	
	Counter-current leaching				
I	1	Leach liquor	142.7	38.3	71.6
	2	Leach liquor	66.1	28.3	
	3	Leach liquor	10.7	4.6	
	Wash water		2.9	0.4	
II	1	Leach liquor	152.3	36.9	68.2
	2	Leach liquor	77.1	28.4	
	3	Leach liquor	6.5	2.7	
	Wash water		0.8	0.2	

Low leaching efficiency can be explained by Si co-dissolution. According to the literature analysis, Si and hot concentrated H_2SO_4 form colloidal particles of SiO_2 (40–100 nm):

$$Si + 2H_2SO_4 \leftrightarrow SiO_2 + 2H_2O + 2SO_2 \quad (1)$$

Particles of SiO_2 form sols, and the surface of the colloidal particles, as a result of dissociation, has a negative charge. The structure of the micelles of hydrosol SiO_2 is as follows:

$$\left\{m[SiO_2]\cdot nSiO_3^{2-}\cdot 2(n-x)H^+\right\}2xH^+ \quad (2)$$

where SiO_3^{2-} ions are potential ions and a $2(n-x)H^+$ ion-adsorbed layer is that in an electrostatic field that moves together with the kernel. $2xH^+$ ions form diffusion layer micelles [37].

It can be assumed that forming a silica hydrosol results in chemical and physical constraints on iron dissolution. A probable mechanism involves the electrostatic adsorption of positively charged iron species onto the negatively charged surface of the silica gel. Moreover, gel formation increases the viscosity of the leach solution, reducing mass transfer rates and limiting the diffusion of iron ions between the solid and liquid phases.

To address this issue, acid regeneration through membrane filtration was investigated. Pilot-scale tests were conducted both to produce SLS for the filtration experiments and to evaluate leaching performance.

3.2. Pilot Scale Tests

After the lab-scale experiments, the best operating conditions were applied to the pilot-scale tests. The pilot plant was housed in a 40 ft standard container, already used for another research project (see Figure 5). The plant is composed of two 500 L polypropylene reactors mechanically stirred; filtration is carried out by a plate-and-frame filter, where the solid cake can also be washed by water. One scrubber treats the gaseous emissions arising from the reactors and assures the change in air. An electrolytic cell is also installed for other processes to test. Figure 6 reports the flow diagram of the plant: storage tanks 2, 3, 4, and the NF unit must be installed outside the container and connected with flexible pipes.



(**a**) (**b**)

Figure 5. Pilot-scale plant: (**a**) plate-and-frame filter and storage tank 1; (**b**) electrolytic cell and reactor 1.

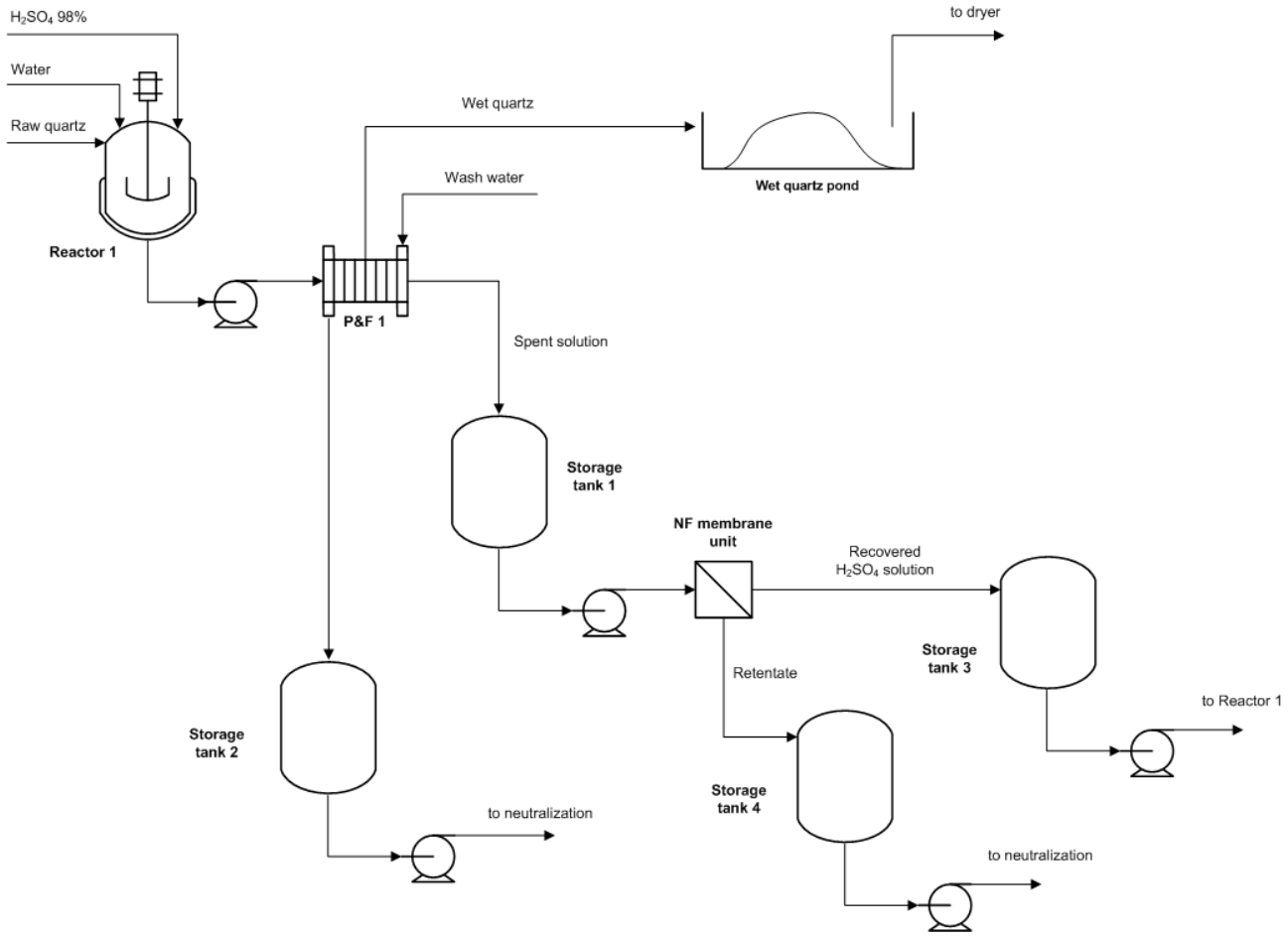


Figure 6. Configuration of pilot plant direct leaching section.

3.3. Membrane Filtration

The importance of acid regeneration in sulfuric acid leaching of quartz lies in its ability to sustain process efficiency, reduce costs, and minimize environmental impact. Regeneration enables recovery of free H_2SO_4 from spent leach solutions, lowering fresh acid consumption while preventing the accumulation of dissolved Fe and silica that would otherwise impair leaching performance. By maintaining the required acid strength, regeneration ensures effective removal of iron impurities, preserves quartz yield, and safeguards product purity. At the same time, it reduces wastewater generation and avoids excessive solid waste production, thereby promoting a closed-loop, environmentally sustainable process suitable for high-purity quartz production.

A total of 5 L of SLS produced in a pilot-scale test was sent to OSMO Membrane Systems, Germany (www.osmo-membrane.de, accessed on 27 September 2025) for lab-scale tests. The membrane module used in the experimental tests is shown in Figure 7.

The flat-channel module has a hydraulic character similar to the most common spiral wound element. Because of that, it is possible to scale up the laboratory test to the pilot scale. The flat cell is equipped with a 44 mil Spacer. On the permeate side is a permeable sintered plate, which has similar characteristics to the permeate spacers and makes the optimal, steady drain of the permeate possible. "MemCell" laboratory tests are allowing evaluations of the process, particularly in relation to the quality of the separation.

In the test, 4.5 L of the spent leaching solution after the direct leaching process was used as a feed solution for a sulfate separation process. The aim of the test was to separate the sulfate, iron, and silica (concentrate side of the process) from the feed solution, and the free acid will pass the membrane (permeate side of the process). The used membrane

was an acid-resistant process membrane (polymeric). The installed membrane area was 160 cm^2. Before starting with the medium from the client, the membrane was compacted at the working pressure for 1 h, and after that, a water equivalent with demineralized water was taken.

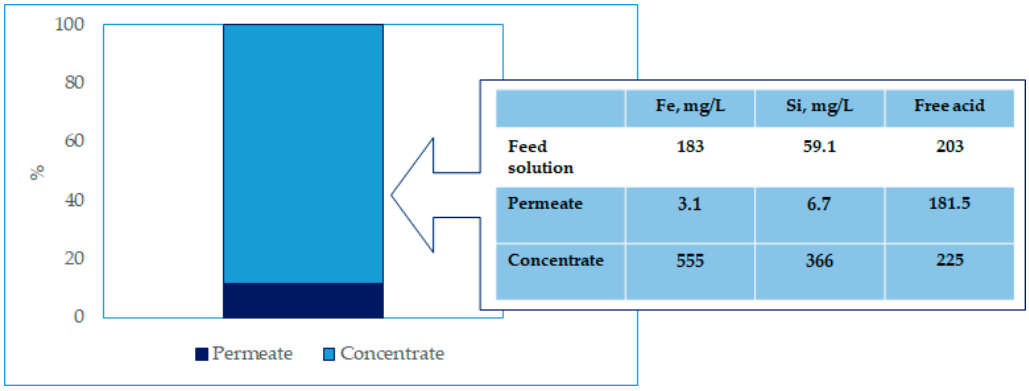


Figure 7. Laboratory test plant "Auto-MemCell".

A pressure of 50 bar was chosen as the working pressure. The whole test was realized at a constant room temperature. To estimate the performance of the separation, a representative value of water was taken with deionized water before and after the test. The permeate was unchanged.

A total of 4.5 L of spent sulfuric acid was separated into 0.517 L of concentrate and 3.983 L of permeate, which means 89% permeate recovery (Volume Concentration Factor: 8.7). The reached fluxes ranged from approx. 30 in the beginning, down to 22 $L/m^2 \cdot h$ in the end.

The analyses of the feed solution, permeate, and retentate were carried out at the laboratories of the University of L'Aquila by ICP. The results are shown in Figure 8.



	Fe, mg/L	Si, mg/L	Free acid
Feed solution	183	59.1	203
Permeate	3.1	6.7	181.5
Concentrate	555	366	225

Figure 8. Effectiveness of membrane process.

After the test, the test plant was flushed with water, and the clean water flux was measured with nearly 100% of the initial value. This means no precipitation or fouling has happened during the test. About 86% of the free acid was recovered in the permeate.

As can be noticed, both iron and silica were removed quantitatively, so that the spent solution can be used again for another leaching stage. Obviously, the membranes shall be tested in a continuous operating mode in order to understand the durability and the replacement time (and thus the operating costs of the RO module).

The resulting solution after membrane filtration was used in the counter-current leaching tests with a make-up of fresh H_2SO_4 to bring back the solution volume to the initial one. The modified scheme and results of the experiments are shown in Figure 9. The analysis of the iron content of the quartz sample before and after three steps of CCL with sulfuric acid regeneration by membrane filtration is presented in Table 5. Elements with concentrations below 0.05% were excluded from the analysis.

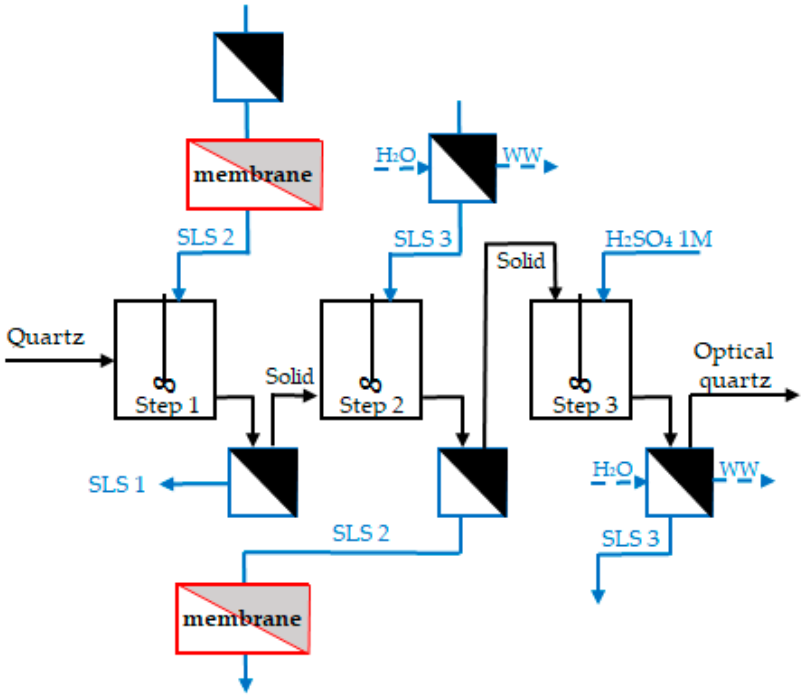


Figure 9. Modified counter-current leaching with SLS regeneration. The blue color in the scheme refers to the liquid flow, and black indicates the solid flow. The red highlights the new additional step in the process. The shaded area represents the filtration process.

Table 5. Chemical composition of sample of studied quartz before and after treatment.

Run	Fraction, μm	Ratio, %	Content								
			Fe	SiO_2	Al_2O_3	TiO_2	CaO	MgO	Na_2O	K_2O	L.O.I
			mg/kg	(%)							
Initial quartz	−1200		668	98.4	0.88	0.056	0.06	0.09	0.15	0.11	0.15
	−1200 + 700	20									
	−700 + 300	30.87									
	−300 + 106	30									
	−106	19.13									
Quartz after treatment	−1200		76	98.4	0.56	0.038	0.02	0.03	0.13	0.05	0.15
	−1200 + 700	18.01									
	−700 + 300	32.48									
	−300 + 106	29.9									
	−106	19.61									

Incorporating a membrane filtration step after the second leaching stage for SLS regeneration increased the overall iron removal efficiency from 70.1% to 88.7% (three independent experiments, standard deviation 1.6%), yielding high-grade quartz.

4. Discussion

The aim of this study was to remove Fe impurities from quartz to obtain high-grade quartz with an iron oxide content below 100 mg/kg. Three different strategies were investigated.

The direct leaching experiments showed that high temperature (90 °C) and a sulfuric acid concentration of 2 M were required. However, even under these conditions, achieving the minimum required Fe removal of 85%—essential for producing high-grade quartz—was not possible.

The cross-leaching tests revealed a dramatic decrease in the leaching solution's effectiveness after the first stage, with an average Fe removal of only 56.4%. This can be attributed to the partial dissolution of quartz under acidic conditions, particularly at elevated temperatures. The dissolved silica forms a protective layer around quartz grains, hindering acid access and limiting further Fe removal.

To reduce sulfuric acid molarity and minimize reagent consumption, the cross-current leaching (CCL) tests were performed using 1 M H_2SO_4. Even with a three-step CCL, the maximum Fe removal achieved did not exceed 70%.

To address the negative effects of silicon co-dissolution, acid regeneration via membrane filtration was investigated. The results confirmed the selectivity of this method, allowing recovery of sulfuric acid while simultaneously removing Fe and Si impurities. Incorporating a membrane filtration step by reusing regenerated sulfuric leaching solution (SLS) after the second step of counter-current leaching with make-up of leaching solution by H_2SO_4 improved Fe removal efficiency from 71.6% to 88.7%.

Process analysis was conducted based on laboratory-scale experiments, including direct leaching, three-step cross leaching, and the first cycle of three-step CCL (Table 6).

Table 6. Comparison of leaching process schemes in quartz purification.

	Direct Leaching	**Cross Leaching**	**Counter-Current Leaching (Regime)**	
			Without Acid Regeneration	**With Acid Regeneration and Make-up of Fresh H_2SO_4**
Effectiveness of the process				
Fe removal, %	80.5	56.4	71.6	88.7
Process parameters				
Step	1	3	3	3
Temperature, °C	90	90	90	90
Solid ratio, % wt/vol	10	10	10	10
Leaching time, h	3	9	3	3
H_2SO_4 concentration, mol/L	2	2	1	1
Reagents consumption for leaching, kg/t of quartz				
H_2SO_4, 98%	687.7	229.2	343.8	381.6
Water	5445.0	2722.7	2722.5	3021.9
Washing water	3066.5	9199.5	3066.5	3066.5
Total	9199.2	12,151.4	6132.8	6470.0
Sustainable recycling				
Acid regeneration, %	0	0	0	33
Acid recycling, %	0	0	66	66

As shown in Table 6, regeneration of the spent leaching solution by membrane filtration increased the effectiveness of CCL from 71.6% to 88.7%, thereby enabling the production of high-purity quartz with an iron content below 100 mg/kg. Moreover, implementing the CCL approach instead of conventional direct leaching reduced acid consumption by nearly 50% and water consumption by 1.4-fold. It increases process efficiency and contributes significantly to environmental protection by minimizing chemical usage, reducing wastewater generation, and promoting resource sustainability.

5. Conclusions

Salient features of the observed phenomena can be explained by silicon dissolution during sulfuric acid leaching, which limits quartz yield, purity, and process efficiency. Neither direct nor cross-leaching could achieve the required effect of iron removal necessary for obtaining high-purity quartz.

Membrane filtration enabled the selective regeneration of sulfuric acid and removal of Fe and Si. The integration of regenerated acid into counter-current leaching enhanced Fe removal from 70.1% to 88.7%, thereby reducing the Fe content in the sample from 668 mg/kg to 76 mg/kg.

The optimized operating conditions for the three-step counter-current leaching configuration were determined to be a temperature of 90 °C, solid-to-liquid ratio of 10% wt/vol, time of 3 h, and H_2SO_4 concentration of 1 M. In this process, the nanofiltration (NF)-regenerated acid and the leaching solution volume were integrated by make-up of fresh H_2SO_4 after each step. In conclusion, integrating membrane-based acid regeneration and counter-current leaching has proved to be an effective method to produce high-purity quartz with the virtuous side effects of acid economization and reduced environmental impact.

In conclusion, integrating membrane-based acid regeneration and counter-current leaching has proved to be an effective method to produce high-purity quartz with the virtuous side effects of acid economization and reduced environmental impact. This approach aligns with several United Nations Sustainable Development Goals: SDG 6 (Clean Water and Sanitation), by minimizing water consumption; SDG 9 (Industry, Innovation, and Infrastructure), through the adoption of innovative membrane technology for process intensification; SDG 12 (Responsible Consumption and Production), via more efficient use of acid and resources; and SDG 13 (Climate Action), by reducing the environmental footprint and associated emissions of the quartz processing operations.

Author Contributions: Conceptualization, F.F. and S.Z.; methodology, N.M.I.; validation, S.Z. and F.F.; formal analysis, I.B.; investigation, I.B.; resources, F.V.; data curation, S.Z.; writing—original draft preparation, S.Z.; writing—review and editing, S.Z. and F.F.; visualization, V.I.; supervision, F.V.; project administration, F.F. All authors have read and agreed to the published version of the manuscript.

Funding: This research received no external funding.

Institutional Review Board Statement: Not applicable.

Informed Consent Statement: Not applicable.

Data Availability Statement: The original contributions presented in this study are included in the articlel. Further inquiries can be directed to the corresponding author.

Conflicts of Interest: The authors declare no conflict of interest.

Abbreviations

The following abbreviations are used in this manuscript:

XRF	X-ray fluorescence analysis
LS	Leaching solution
SLS	Spent leaching solution
CCL	Counter-current leaching
WW	Washing water
HPQ	High-purity quartz

References

1. Zhang, R.; Tang, C.; Ni, W.; Yuan, J.; Zhou, Y.; Liu, X. Research Status and Challenges of High-Purity Quartz Processing Technology from a Mineralogical Perspective in China. *Minerals* **2023**, *13*, 1505. [CrossRef]
2. Prasetyo, A.B.; Handayani, M.; Sulistiyono, E.; Firdiyono, F.; Febriana, E.; Mayangsari, W.; Wahyuningsih, S.; Pramono, E.; Maksum, A.; Riastuti, R.; et al. Fabrication of High Purity Silica Precipitates from Quartz Sand toward Photovoltaic Application. *J. Ceram. Process. Res.* **2023**, *24*, 103–110. [CrossRef]
3. Long, H.; Zhu, D.; Pan, J.; Li, S.; Guo, Z.; Xu, X. Innovative process for the extraction of 99.99% high-purity quartz from high-silicon iron ore tailings. *J. Mater. Res. Technol.* **2024**, *31*, 2094–2102. [CrossRef]
4. Liu, C.; Wang, W.; Wang, H.; Zhu, C.; Ren, B. A Review on Removal of Iron Impurities from Quartz Mineral. *Minerals* **2023**, *13*, 1128. [CrossRef]
5. Zhan, L.; Wang, Q.; Ku, J.; Shang, H.; Shen, Z. Purification Technologies for High-Purity Quartz: From Mineralogy to Applications. *Sep. Purif. Rev.* **2025**, 1–18. [CrossRef]
6. Wang, L.; Wang, G.D.; Ge, P.; Sun, W.; Tang, H.H.; Hu, W.J.H. Activation mechanisms of quartz flotation with calcium ions and cationic/anionic mixed collectors under alkalescent conditions. *Colloid Surf. A* **2022**, *632*, 127771. [CrossRef]
7. Dai, P.; Yang, J.; Wei, Z.; Zeng, J.; Xue, Z.; Chen, L. Magnetic properties of chalcopyrite and arsenopyrite for high-gradient magnetic separation with Crystal-Field Theory. *Miner. Eng.* **2022**, *189*, 107893. [CrossRef]
8. Li, Y.K.; Li, S.Q.; Pan, X.D.; Zhao, X.; Guo, P.H. Pre-concentration of quartz from sea sand through superconducting high gradient magnetic separation technology. *Sep. Sci. Technol.* **2023**, *58*, 822–834. [CrossRef]
9. Quartz Gravity–Magnetic Separation Combined Process: A Step-By-Step Guide—Xinhai. 2025. Available online: www.xinhaimining.com/newo/quartz-gravity-magnetic-separation-combined-process.html (accessed on 22 October 2025).
10. Haghi, H.; Noaparast, M.; Shafaei Tonkaboni, S.Z.; Mirmohammadi, M. A New Experimental Approach to Improve the Quality of Low Grade Silica; The Combination of Indirect Ultrasound Irradiation with Reverse Flotation and Magnetic Separation. *Minerals* **2016**, *6*, 121. [CrossRef]
11. Wang, M. The Experiment of Scrubbing and Purifying a Quartz Mine. *Hunan Nonferrous Met.* **2020**, *36*, 20–23.
12. Shao, H.; Zang, F.; Ji, M.; Yu, M. Prepare and mechanism of high purity quartz by alkali corrosion and acid leaching process using vein quartz. *Silicon* **2022**, *14*, 12475–12483. [CrossRef]
13. Zheng, R.; Ren, Z.; Gao, H.; Zhang, A.; Bian, Z. Effects of calcination on silica phase transition in diatomite. *J. Alloys Compounds* **2018**, *757*, 364–371. [CrossRef]
14. Long, H.; Zhu, D.; Pan, J.; Li, S.; Yang, C.; Guo, Z. Advanced processing techniques and impurity management for high-purity quartz in diverse industrial applications. *Minerals* **2024**, *14*, 571. [CrossRef]
15. Liu, Y.; Xie, Y.; Tian, S. Study on the whitening effect and mechanism of alkali-additive-enhanced roasting on low-whiteness barite. *Miner. Eng.* **2025**, *234*, 109711. [CrossRef]
16. Yu, Z.; Luo, D.; Zhao, K.; Rong, K.; Deng, J.; Gao, Z. High-purity quartz sand from mineral purification: A review on process, mechanism, and environmental strategies. *Miner. Eng.* **2026**, *235*, 109801. [CrossRef]
17. Martins Benetti, R.; de Souza-Pereira, M.; Cardoso Bellettini de Souza, G.; Elyseu, F.; Jaramillo-Nieves, L.J.; Bernardin, A.M. Whitening of kaolin-quartz-feldspar dental porcelains by chemical attack using commercial peroxides. *Next Mater.* **2025**, *6*, 100498. [CrossRef]
18. Ma, Y.; Li, J.; Wu, Z.; Zhang, H.; Tan, X.; Yi, Y.; Tan, Q.; Liu, Q. Characteristics of high-purity quartz raw materials for crucibles and exploration of key purification technologies. *Miner. Eng.* **2025**, *231*, 109446. [CrossRef]
19. Shuai, H.; Yang, X.; Xu, X.; Du, G.; Wang, J. Mechanochemical effect assisted oxidative whitening of black talc. *Appl. Clay Sci.* **2025**, *277*, 107961. [CrossRef]
20. Zhong, Y.; Fang, Q.; Wei, Z.; Li, Y. Experimental Study on Preparation of High-purity Quartz Sand from Typical Quartz Resources in South Jiangxi. *Nonferrous Met.* **2025**, *7*, 122. [CrossRef]
21. Bonifazi, G.; Grosso, G.; Palmieri, R.; Serranti, S. Current trends and challenges in construction and demolition waste recycling. *Curr. Opin. Green Sustain. Chem.* **2025**, *53*, 101032. [CrossRef]

22. Bonifazi, G.; Palmieri, R.; Serranti, S. Evaluation of attached mortar on recycled concrete aggregates by hyperspectral imaging. *Constr. Build. Mater.* **2018**, *169*, 835–842. [CrossRef]
23. Zhang, Z.; Li, J.; Li, X.; Huang, H.; Zhou, L.; Xiong, T. High efficiency iron removal from quartz sand using phosphoric acid. *Int. J. Miner. Process.* **2012**, *114–117*, 30–34. [CrossRef]
24. Ubaldini, S.; Piga, L.; Fornari, P.; Massidda, R. Removal of iron from quartz sands: A study by column leaching using a complete factorial design. *Hydrometallurgy* **1996**, *40*, 369–379. [CrossRef]
25. Hayatullah, A.; Shanti, A.S.; Mostafa, M.G.; Rahman, M.A.; Biswas, P.K.; Alam, M.S.; Rana, M.S.; Uddin, M.R.; Nuruzzaman, M.; Shahrian, M.S.; et al. Iron removal from red clay using oxalic acid leaching for enhanced ceramic industry applications. *Heliyon* **2025**, *10*, e38863. [CrossRef]
26. Vegliò, F.; Passariello, B.; Barbaro, M.; Plescia, P.; Marabini, A.M. Drum leaching tests in iron removal from quartz using oxalic acid and sulphuric acids. *Int. J. Miner. Process.* **1998**, *54*, 183–200. [CrossRef]
27. Ambikadevi, V.R.; Lalithambika, M. Effect of organic acids on ferric iron removal from iron-stained kaolinite. *Appl. Clay Sci.* **2000**, *16*, 133–145. [CrossRef]
28. Arslan, V. The Modeling and Optimization of Iron Removal from Silica Sand Under Ultrasound-Assisted Leaching by Response Surface Methodology. *Min. Metall. Explor.* **2021**, *38*, 2229–2237. [CrossRef]
29. Ibrahim, A.F.M.; Seifelnassr, A.A.S.; Al-Abady, A.; El-Salmawy, M.S.; Abdelaal, A.M. Characterization and Iron Removal Enhancement of El-Zaafarana White Sand. *Min. Metall. Explor.* **2022**, *39*, 2187–2198. [CrossRef]
30. Du, X.; Yang, D.; Zheng, S.; Sun, Z.; Li, C. Deep insight into the reductive roasting treatment on iron removing from quartz. *Adv. Powder Technol.* **2021**, *32*, 4825–4832. [CrossRef]
31. Zhang, H.; Guo, S.; Wu, J.; Wu, D.; Wei, K.; Ma, W. Effect of quartz crystal structure transformations on the removal of iron impurities. *Hydrometallurgy* **2021**, *204*, 105715. [CrossRef]
32. Styriakova, I.; Bekenyiova, A.; Styriakova, D.; Jablonovska, K.; Styriak, I. Second pilot-plant bioleaching verification of the iron removal form quartz sands. *Procedia Earth Planet. Sci.* **2015**, *15*, 861–865. [CrossRef]
33. Suba, J.; Styriakova, D. Iron minerals removal from different quartz sands. *Procedia Earth Planet. Sci.* **2015**, *15*, 849–854. [CrossRef]
34. United Nations. The 17 Sustainable Development Goals. United Nations. 2015. Available online: https://sdgs.un.org/goals (accessed on 22 October 2025).
35. Kefaifi, A.; Sahraoui, T.; Kheloufi, A.; Bobocioiu, E. Optimization of Quartz Sand Leaching Process Using Design Experiments Method (DOE). *Silicon* **2019**, *11*, 1481–1488. [CrossRef]
36. Xia, M.; Yang, X.; Hou, Z. Preparation of High-Purity Quartz Sand by Vein Quartz Purification and Characteristics: A Case Study of Pakistan Vein Quartz. *Minerals* **2024**, *14*, 727. [CrossRef]
37. Ferella, F.; Leone, S.; Innocenzi, V.; De Michelis, I.; Taglieri, G.; Gallucci, K. Synthesis of zeolites from spent fluid catalytic cracking catalyst. *J. Clean. Prod.* **2019**, *230*, 910–926. [CrossRef]

Disclaimer/Publisher's Note: The statements, opinions and data contained in all publications are solely those of the individual author(s) and contributor(s) and not of MDPI and/or the editor(s). MDPI and/or the editor(s) disclaim responsibility for any injury to people or property resulting from any ideas, methods, instructions or products referred to in the content.